NASA Technical Memorandum 4197

Video Camera System for Locating Bullet Holes in Targets at a Ballistics Range

A. W. Burner, D. R. Rummler,
and W. K. Goad
Langley Research Center
Hampton, Virginia

National Aeronautics and
Space Administration
Office of Management
Scientific and Technical
Information Division

1990

Summary

A system consisting of a single charge-coupled-device (CCD) video camera, computer-controlled video digitizer, and software to automate the measurement has been developed for locating bullet holes in targets at a ballistics range at the Langley Research Center. The camera/digitizer system is a crucial component of a highly instrumented, indoor 50-m rifle range that supports the development of wind-resistant ultramatch ammunition. The system was designed to take data rapidly (10 sec between shots) and automatically with little operator intervention. The system description, measurement concept, and procedure are presented along with laboratory tests of repeatability and bias error. The long-term (1-hr) repeatability of the system was found to be 4 μm (one standard deviation) at the target, and the bias error was found to be less than 50 μm. An analysis of the potential errors and a technique for calibration of the system are presented.

Introduction

The purpose of the ballistics range at the Langley Research Center is to support the development of wind-resistant ultramatch ammunition. The facility consists of an indoor 50-m range with instrumented machine rests for rifles and barreled actions. One of the crucial requirements of the instrumentation is the automated location of a bullet hole on a target within ± 100 μm. In the past, the effect of a ballistic variable, such as bullet velocity, on shot-location precision has been determined by measuring the spread of shot groups manually, which is not conducive to the study of the effects.

The recent availability of relatively inexpensive solid-state, charge-coupled-device (CCD), area-array video cameras and computer-controlled video frame digitizers has enabled the automation of the bullet-hole-location measurement. The automation of the measurement will uniquely, and for the first time, enable the correlation of bullet placement with measured ballistic variables and allow computer reconstruction of shot groups. The development of the present system, which uses a single camera and object movement constrained to a plane, was expedited by the development work for a two-camera, three-dimensional (3-D) video photogrammetric system reported in reference 1.

It was desired in the development of the automated video measuring system to use software code that can be easily modified to interface with other required instrumentation, such as chronographs that are used to measure bullet velocities. In addition, it was desired to keep the code flexible enough that a casual programmer, probably experienced only in BASIC, can implement changes and additions to the code as the data acquisition or reduction procedures are changed.

Symbols

c	image distance (camera constant), mm
D_o	distance from origin to camera, m
f	focal length, mm
r	radial image distance, mm
S_X, S_Y	true scale (to convert from image to object)
S_{Xc}, S_{Yc}	calibrated scale
s_h, s_v	pixel spacing, mm
X, Y, Z	true object location, mm
X', Y'	measured object location, mm
X_c, Y_c, Z_c	location of camera perspective center, m
X_o, Y_o	origin offset for transformation, mm
x, y	first-order image coordinates, mm
x', y'	distorted image coordinates, mm
$x_{\text{pix}}, y_{\text{pix}}$	centroid, pixels
$\Delta X, \Delta Y$	spacing of calibration targets in object plane, mm
$\Delta x, \Delta y$	spacing of calibration targets in image plane, mm
δr	radial distortion, mm
θ	rotation angle for transformation, deg
σ	third-order radial distortion coefficient, mm^{-2}
ϕ	camera angle to XY-plane, deg

Abbreviations:

AOI	area of interest
CCD	charge-coupled device
cal	calibration
h	horizontal
rss	root sum square
sag	sagitta of line, mm
v	vertical

Measurement Concept

The measurement concept is simply to use scale, found by independent calibration, to convert from image to object coordinates on the paper-target object plane. This desired scale is equal to the inverse of the lateral magnification commonly used in first-order optics, and it is positive for video images. To avoid being struck by a bullet, the camera will be offset from the normal to the object plane and tilted to center the paper target in its field of view (fig. 1). Thus, the scale will vary across the field of view. This is true even for a perfect system that obeys the first-order (Gaussian) object-image relationships. This variation in scale (sometimes called keystone distortion for the keystonelike image of a rectangular object) is quite separate from the optical aberration of distortion, which is also due to a variation in scale across the image plane. However, the aberration of distortion is nonlinear and can exist even when the optical axis of the camera is normal to the object plane.

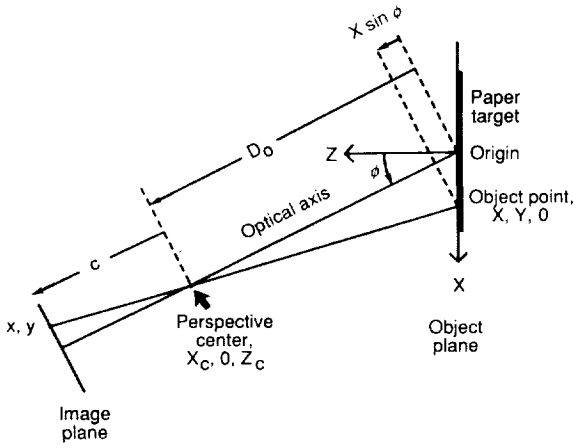

Figure 1. Plan view of measurement geometry.

The scale can be determined as the ratio of a known length in the object plane to its length in the image plane. To partially compensate for differences in scale between two orthogonal axes on the tilted object plane as well as for scaling differences in converting pixels to units of length on the CCD sensor, it was decided to use two fixed scales for X and Y that are determined by calibration.

Taking the paper-target object to be in the XY-plane with the origin at its center, the camera perspective center will be located at X_c, Y_c, Z_c (where $Y_c = 0$) as shown in figure 1. Thus, the camera optical axis will be inclined to the object plane normal (Z-axis) by an angle ϕ given by $\tan^{-1}(X_c/Z_c)$. The perspective center of the camera will be located at a distance D_o from the origin of the object plane given by

$$D_o = (X_c^2 + Z_c^2)^{1/2} \tag{1}$$

It is assumed in much of the following discussion that the camera obeys the first-order object-image relationships. Such an assumption is appropriate and yields a reasonable estimate of performance since imaging devices such as video cameras are designed to closely approximate first-order operation.

There are several equivalent ways to compute scale for a first-order optical system. A convenient relationship for this analysis is that the scale for any plane normal to the optical axis is given by the distance from the object plane to the perspective center (perpendicular object distance) divided by the distance from the perspective center to the image plane (perpendicular image distance). For the geometry of figure 1, the perpendicular object distance for any point on the XY-plane is $D_o - X \sin\phi$. The scale for Y, represented by S_Y, is then given by

$$S_Y = (D_o - X \sin \phi)/c \tag{2}$$

The image distance (or camera constant) c is determined by the focus setting of the camera and, once set, is a constant of the camera independent of object location. Note that for a given setup, D_o, ϕ, and c are constants so that S_Y varies linearly with X with an intercept of D_o/c and a slope of $\sin\phi/c$ and is independent of Y. For a setup in which $\phi = 0, S_Y$ reduces to the familiar object distance D_o over image distance c. The scale for X, S_X, is related to S_Y by

$$S_X = S_Y/\cos \phi \tag{3}$$

and is also independent of Y and varies linearly with X for a given setup. The division by the $\cos\phi$ term is necessary to convert from a length normal to the optical axis to a length along the X-direction of the object plane. The true scales S_X and S_Y in equations (3) and (2), respectively, relate the X, Y object plane coordinates of any point to its image plane coordinates x, y by

$$\left.\begin{aligned} X &= xS_X \\ Y &= yS_Y \end{aligned}\right\} \tag{4}$$

The measurement concept employed here is to replace S_X and S_Y which vary with X with two fixed scales found by calibration, S_{Xc} and S_{Yc}. The calibrated scales are determined by ratioing object-to-image lengths along the X-axis (for S_{Xc}) and along the Y-axis (for S_{Yc}). If S_X and S_Y are replaced with the two fixed-scale values determined by calibration,

the measured object plane coordinates, represented by X' and Y', are given, respectively, by

$$\left.\begin{aligned} X' &= xS_{Xc} \\ Y' &= yS_{Yc} \end{aligned}\right\} \tag{5}$$

Equations (5) are the basic relations used to locate a bullet hole with the object plane error given by $X' - X$ and $Y' - Y$. The calibrated scales S_{Xc} and S_{Yc} are derived from the ratio of known object lengths, ΔX and ΔY, to image lengths, Δx and Δy, respectively, found during a calibration. Thus,

$$\left.\begin{aligned} S_{Xc} &= \Delta X/\Delta x \\ S_{Yc} &= \Delta Y/\Delta y \end{aligned}\right\} \tag{6}$$

The error in using equations (5) instead of equations (4) is presented in the appendix for the expected geometry at the ballistics range. The largest error occurs at the edge of field and is only 3 μm. It thus appears adequate, at least for the geometry expected at the ballistics range, to replace the true scales that vary with X with the two fixed scales found by calibration. The appendix also contains a discussion of error estimates due to camera placement, misalignment of the paper target to the calibration plane, spacing of the calibration targets, measurement errors of the image and object planes, and optical lens distortion. The estimated combined bias error is shown to be 19 μm for the error sources considered. Because of the use of only the central portion of the image area and the partial compensation of the calibration, there is little need to correct for optical distortion.

System Description and Procedure

A layout of the ballistics range with the CCD camera system in place is shown in figure 2. A Cohu model 4815 CCD video camera is mounted on a tripod 2.5 m from the target which is in the XY-plane. (See fig. 1 for the coordinate system referred to.) The video camera is displaced from the Z-axis by 0.3 m. The paper-target object plane is located behind a reference surface that has two pairs of circular targets separated in the X- and Y-directions by approximately 100 mm. The targets on the reference surface establish a relative center from which the location of a bullet hole is measured, and they are used to correct for the relative movement between the camera and paper target as well as for camera image drifts that can occur during warm-up or temperature changes.

The two pairs of targets on the reference surface can be used to determine the scale in the X- and Y-directions instead of using a separate calibration plate if compensation is made for the displacement of the reference surface from the paper-target object

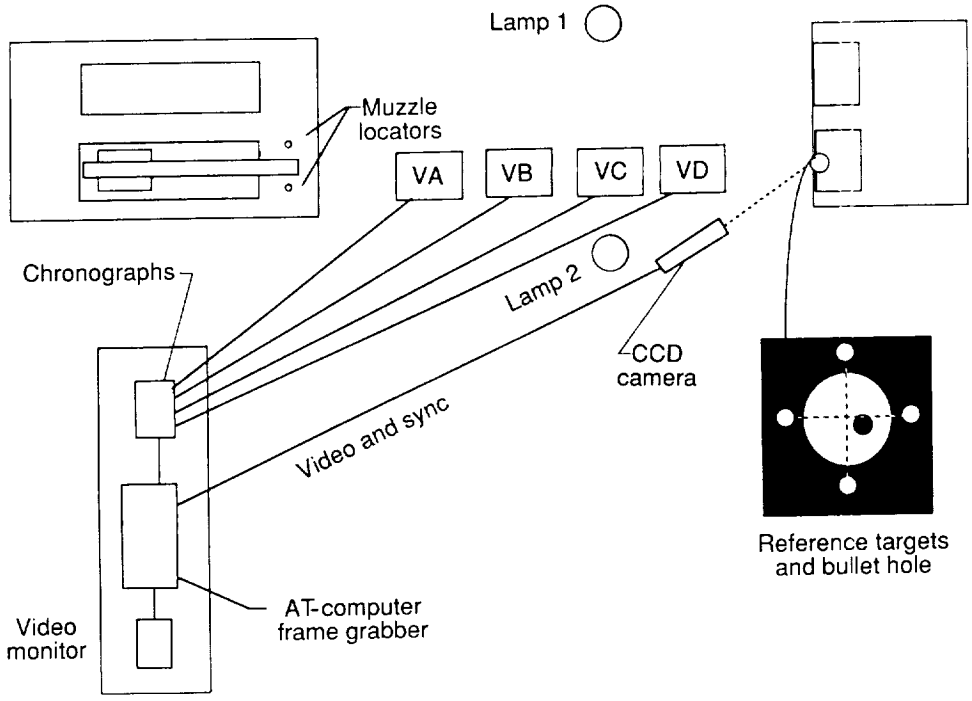

Figure 2. Plan view of ballistics range with CCD camera system in place. VA, VB, VC, and VD denote velocity stations.

plane. However, tests using only the reference surface for calibration had larger errors than tests using a separate calibration plate located in the plane of the paper target with closer spaced targets (25 mm). It was thus decided to include in the procedure a calibration with a separate calibration plate that is then removed before a shooting session is started. The four targets on the reference surface are then used simply to establish the center of the target plane during the shooting session.

The camera CCD sensor has 754 (horizontal) pixels by 484 (vertical) pixels with pixel dimensions of 11.5 (h) μm by 27.0 (v) μm. The photointegration site is shifted electronically 1/2 pixel in the vertical direction between video fields to yield an effective vertical pixel spacing of 13.5 μm for the full video frame. The video camera lens has a focal length of 75 mm and is mounted on an attachment that doubles the focal length to 150 mm.

The composite video output from the camera is input to an Epix Silicon Video frame-grabbing and digitization board with 1 Mbyte onboard storage which resides in an 8-MHz AT-class computer. The video camera is synchronized by the Epix board. An analog video output from the Epix board displays the digitized images on a monitor. A video frame is digitized by the Epix board into 752 (h) by 480 (v) pixels with 256 gray levels. Since the clocks of the camera and Epix board are at the same nominal frequency (14.318 MHz), the effective horizontal and vertical pixel spacings for the camera/digitizer system and camera alone will be nearly equal. Differences between the system and camera pixel spacings will be partially compensated by the calibration scales, S_{Xc} and S_{Yc}. Calibration procedures and considerations for measuring the effective horizontal and vertical pixel spacings are found in reference 1.

Commands to set up the Epix board, grab and digitize the video signal, perform image-processing operations, and store digitized video frames can be developed as text command files to perform multiple operations from within the executable code supplied by the manufacturer. For this particular application it was convenient to use the BASIC SHELL command to return to the disk operating system (DOS) and execute the Epix software (written in C) to perform various operations and then to exit to the BASIC code for further processing. With this procedure, command files to cause the Epix board to perform various operations can be created within BASIC before "SHELLing" out to run the Epix code.

Any values such as pixel locations that are only outputted to the computer screen by the Epix code can be read from the screen with BASIC and used for further computations or operations. The Microsoft QuickBASIC 4.0 environment was chosen for code development because of its interpreterlike operation, full-screen editing, and rapid compilation and execution of code. Digitized image files are stored on a virtual disk (RAM) which decreases the amount of time taken for image storage and retrieval and also decreases the time taken for the random access file reads required to compute gray level centroids in BASIC.

A simplified flowchart for the computer code is presented in figure 3. A new shooting session is begun by reading the calibration data and the locations in pixels of the reference targets, all of which are stored on file from the last session. A command file is then created within BASIC which, with the SHELL command, can be used to digitize a full-resolution image and overlay the output video image with crosses at the last locations of the reference targets (fig. 4). This is to determine whether gross movement has occurred between sessions that would require manual recentering on the reference targets or possible recalibration. Options are then presented to the user to (1) take data automatically, (2) take data manually, (3) enable or disable the automatic centroiding of the reference targets, (4) perform a calibration, (5) display crosses on the reference targets, or (6) quit the session.

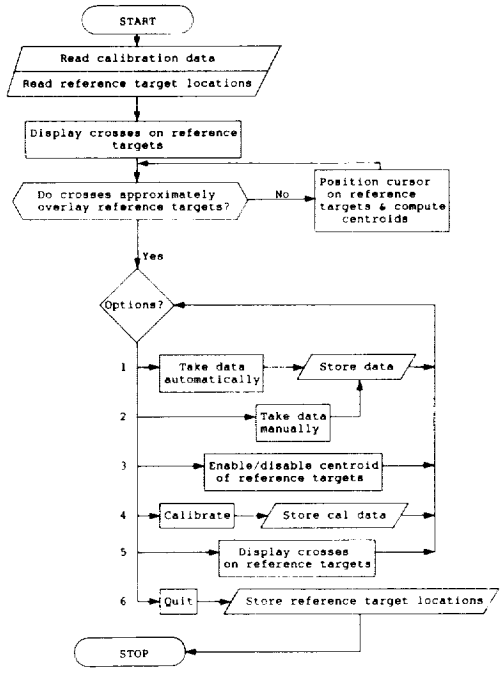

Figure 3. Simplified flowchart of computer code.

For initial tests, or if the camera or target plane has moved, it is necessary to place the calibration plate with its front surface in the plane of the paper

target in order to determine new values of S_{Xc} and S_{Yc}. The aluminum calibration plate has two pairs of circular targets separated along the X- and Y-axes by 25 mm. Two quartz-halogen 300-W lamps are positioned to provide approximately uniform illumination. If the calibration option is chosen, a video image is grabbed, digitized, and displayed on the video monitor along with a cursor that must be positioned (to within a few pixels) to the four calibration targets in the designated sequence.

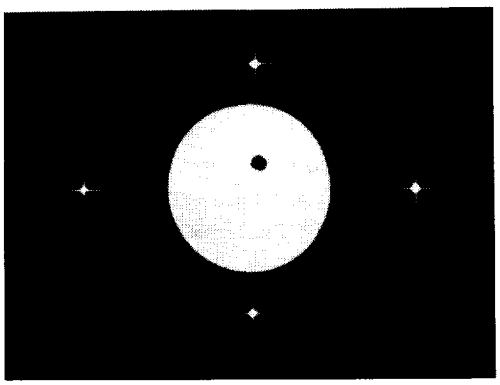

(a) Crosses displayed on reference targets at startup of shooting session.

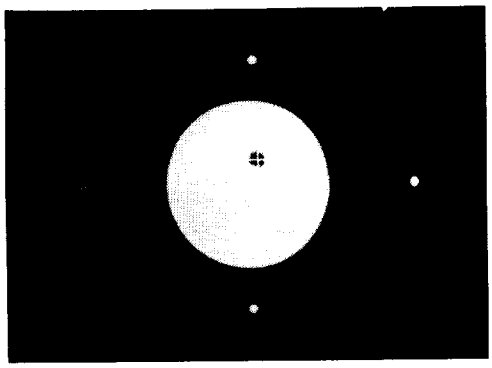

(b) Cross displayed on bullet hole location found during shooting session.

Figure 4. Video monitor displays.

Once the four calibration targets have been located, the gray level centroid is computed (in BASIC) for each target after an automatic background subtraction. The gray level background automatically subtracted is the maximum gray level on the perimeter of a 35- by 35-pixel area-of-interest (AOI) surrounding the location of the target found manually. The origin of the pixel coordinates is in the upper left of the digitized image with positive x to the right and positive y downward. The gray level centroids in pixels $(x_{\text{pix}}, y_{\text{pix}})$ are transformed to millimeters on the image plane with

$$\left.\begin{aligned} x &= (x_{\text{pix}} - 376)s_h \\ y &= (240 - y_{\text{pix}})s_v \end{aligned}\right\} \tag{7}$$

where s_h is the horizontal pixel spacing equal to 11.5 μm and s_v is the vertical pixel spacing equal to 13.5 μm. Equations (6) are then used to compute S_{Xc} and S_{Yc} which are stored in a calibration file for use in future sessions.

After performing the calibration and removing the calibration plate, the paper-target transport is positioned behind the reference surface at the calibration plane. To simplify the measurement and avoid the possibility of overlapping bullet holes in a target, only one bullet hole is allowed in the field of view of the video camera at a time. To accomplish this the paper target is translated between rounds. At present, the automatic measurement of the location of the bullet hole is initiated with a carriage return. In the future, it is expected that a trigger will be derived from the velocity instrumentation to initiate data acquisition after sufficient delay to allow any paper-target vibration to cease.

The automatic measurement of the bullet hole location is begun by digitizing and storing a full-resolution image on the Epix video board. The gray level contrast is next reversed for a 174- by 152-pixel AOI with the center determined by the targets on the reference surface. The contrast reversal is necessary since the bullet hole is a black target on a white background. The contrast-reversed AOI is then stored on virtual disk. Before exiting the Epix code, the contrast-reversed AOI is enhanced and the binary centroid is computed. The binary centroid is used as the start location for the gray level centroid which is computed after returning to the BASIC code. If reference target centroiding is enabled, then 32- by 28-pixel AOI's surrounding the last centroid locations of the four reference targets are also digitized and stored on virtual disk.

After returning to the BASIC code, the gray level centroid of the bullet hole within a 40- by 40-pixel AOI is computed with the center determined by the binary centroid; and if reference target centroiding is enabled, the gray level centroids of the four reference targets are also computed. The centroid in pixels of the bullet hole is converted to millimeters on the image plane with equations (7). The target center given in millimeters on the image plane, as

determined from the intersection of the pair of lines formed by the four reference targets (see fig. 2), is subtracted from the image coordinates before applying equations (5) to determine the object plane coordinates of the bullet hole. A cross is displayed on the current image at the location of the bullet hole centroid to verify proper operation (fig. 4). With an 8-MHz AT-class computer, the time required for the automated measurement is 8 sec when reference centroiding is disabled and 12 sec when enabled.

If reference target centroiding is enabled, then the target center is recomputed for each measurement of the bullet hole location using the latest centroid values for the four reference targets. Thus, camera movement or drift due to temperature changes is compensated. In addition, the reference target scale ratio in X and Y for each shot compared with that at calibration is used to multiply S_{Xc} and S_{Yc}. In this way, small camera movements in the Z-direction (which cause corresponding changes in S_{Xc} and S_{Yc}) are partially compensated even though the reference surface is displaced from the calibration plane. This is because changes in S_{Xc} and S_{Yc} are only weakly dependent on the actual value of Z.

If the manual option is selected, a full-resolution image is digitized and stored on the Epix board and a cursor is displayed for manual setting on the bullet hole. Based on the manual setting, the gray level centroid of a 35- by 35-pixel AOI is made and the computation of the bullet hole location then proceeds as above for the automated measurement.

Laboratory Tests

Laboratory tests were conducted to establish the repeatability and bias error of the system. The repeatability tests establish a lower limit on error when data are taken only once and also indicate, based on comparisons with independent bias error estimates or tests, whether it is advantageous to take multiple data for a single bullet hole. The bias error of the system was determined based on known positioning of a bullet hole in two dimensions with high-precision translation stages. In addition, simple tests were made of the effects of lighting variations on the measurement.

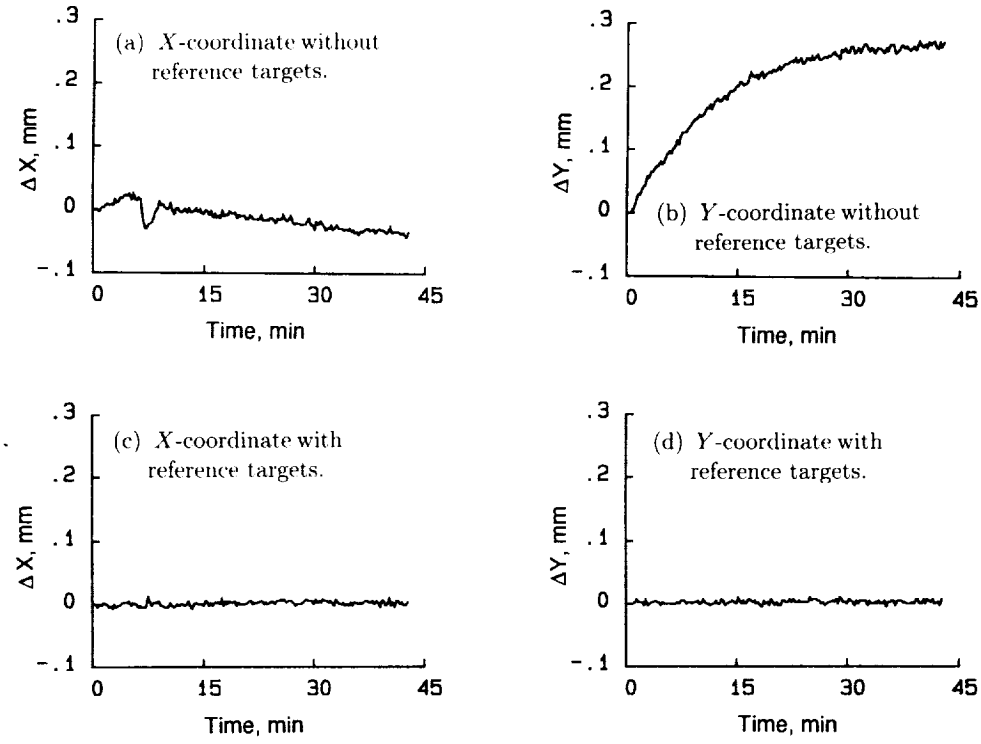

Figure 5. Repeatability tests of CCD camera system for a stationary bullet hole during warm-up. Variations in X- and Y-coordinates are shown without and with reference targets.

Repeatability Tests

For the repeatability tests a paper target with a 0.22-caliber bullet hole in it was positioned in a fixed location behind the reference surface with the camera located 2.5 m away and offset from the Z-axis by 0.3 m. A timing loop was set up within the BASIC code to automatically record data every 15 sec. Tests were conducted both during warm-up and after warm-up. For the tests during warm-up, the camera was turned on for 30 sec before data acquisition was started. For the repeatability tests after warm-up, the camera had been on almost 3 hr before data acquisition was initiated. For both tests, the targets on the reference surface as well as the bullet hole were centroided and the data were recorded as a function of time. The usefulness of the reference targets could then be determined by computing the bullet hole location as a function of time both with and without use of the reference targets to redetermine the relative center of the paper target and scales.

The warm-up repeatability results are presented in figure 5. In figures 5(a) and 5(b) the variations in the X and Y object plane coordinates of the bullet hole are plotted as a function of time without using the reference targets to redetermine the relative center or correct the scales. The first coordinates computed were subtracted from the data to determine the coordinate variations for the plots. The slight increase in the X-coordinate initially, the sudden dip at about 6 min, and the gradual decrease afterwards are characteristic of centroids taken along the x-axis of the camera as noted in repeat tests. The X-coordinate range was 65 μm. The exponential increase in the Y-coordinate is characteristic of centroids taken along the y-direction of the camera and is given by

$$\Delta Y \approx 265(1 - e^{-t/10}) \tag{8}$$

where t denotes time and is given in minutes and ΔY is given in micrometers. The equivalent vertical shift in pixels in the $+y$-direction of the image plane during warm-up is -1.2 pixels. (The negative sign is due to the sign convention for y in pixels.) With a time constant of 10 min, ΔY will be within 3 μm of the peak value of 265 μm after about 45 min, which is considered to be the minimum warm-up time for image stability to a fraction of a pixel.

In figures 5(c) and 5(d) the variation in object plane coordinates is given when the four reference targets are used to establish the relative center and adjust the scales. The large variations noted in figures 5(a) and 5(b) are then reduced to a standard deviation of 3.7 μm with a range of 20 μm for X and a standard deviation of 3.2 μm and a range of 15 μm for Y. The ranges in figures 5(a) and 5(b) have been reduced by using the reference targets by a factor of 3.3 in X and a factor of 17.7 in Y. Nearly all improvement is attributable to the adjustment of the relative center rather than to scale adjustments. (The variations in object plane coordinates caused by scale changes in the two pairs of reference targets have a standard deviation at the edge of a 16- by 16-mm object field of only 0.7 μm and a range of 4.3 μm in both X and Y based on computations of the adjusted scales of the four reference targets as a function of time.)

After the camera has been operating for 3 hr, the standard deviations of the X- and Y-coordinates of the stationary bullet hole for data taken over a 1-hr period reduce to 6.9 μm with a corresponding range of 36 μm in X and to 6.6 μm with a corresponding range of 46 μm in Y if the four reference targets are not used to recompute the relative center (fig. 6). In figure 6 the mean values of X or Y computed using the four reference targets are subtracted from the data sets before plotting. Just as for the tests during camera warm-up, the variations in the x- and y-axis centroids of the four reference targets closely follow those of the bullet hole so that when the four reference targets are used to recompute the relative target center, the standard deviations reduce to 4.1 μm in X and to 3.3 μm in Y with ranges of 21 μm and 18 μm, respectively. These values are not statistically different from the standard deviations computed for figures 5(c) and 5(d). Thus, providing reference target centroiding is enabled, the stability of the system is maintained throughout the warm-up period of the camera.

Bias Error Tests

The bias error of the bullet hole measuring system was determined with two high-resolution (0.1 μm) computer-controlled translation stages arranged to move the bullet hole in the XY-plane over a 16- by 16-mm object field. The single-axis uncertainty of the stages over 16 mm of travel was determined to be ± 5 μm by comparison with a distance-measuring laser interferometer. The translation stages were used to position the bullet hole at 49 points covering the field of view. The locations computed with the CCD camera system were then transformed to the known stage locations by nonlinear least squares using the following conformal transformation with offset X_o,Y_o in which the scale is forced to be 1:

$$\left.\begin{aligned} X' &= X \cos\theta + Y \sin\theta + X_o \\ Y' &= Y \cos\theta - X \sin\theta + Y_o \end{aligned}\right\} \tag{9}$$

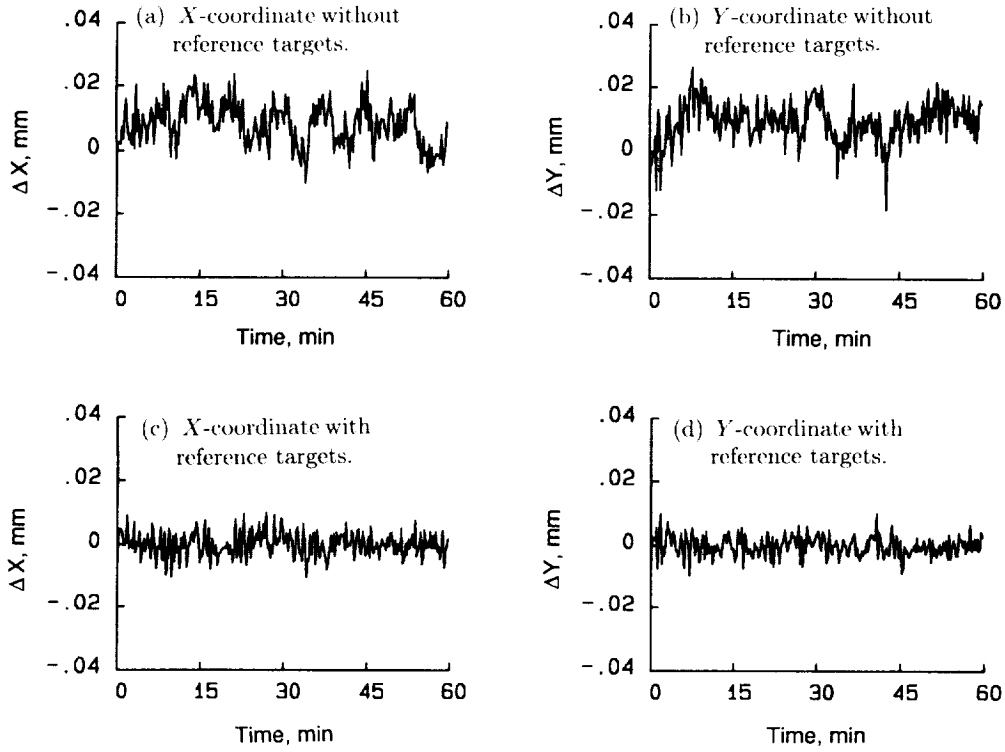

Figure 6. Repeatability tests of CCD camera system for a stationary bullet hole after warm-up. Note change of scale from figure 5.

This transformation simply removes any rotation or origin shift between the CCD camera system coordinates and the two-dimensional (2-D) stage coordinates. Thus, the residuals found after transformation represent the differences between the two measurements without additional arbitrary bias errors due to rotation or origin shift of the coordinate systems.

The root-mean-square residuals in the object plane were 25 μm in X and 30 μm in Y with maximum residuals of 48 μm in X and 43 μm in Y. The residuals after transformation with equations (9) are plotted in figure 7. A conservative estimate of bias error is taken to be 50 μm in both X and Y. Since the experimentally determined bias error is less than the initial requirement by a factor of 2, the discrepancy between the experimental bias error and predicted bias error (see the appendix) was left unresolved. The discrepancy is likely due to residual image plane distortions larger than the 1 μm used for the prediction in the appendix. Another source for the discrepancy could be 2-D translation errors in the stages used to move the bullet hole for the experimental tests. Also note that the acquisition of multiple images at a single bullet hole location is not necessary except to verify system stability because of the small value of the repeatability compared to bias error.

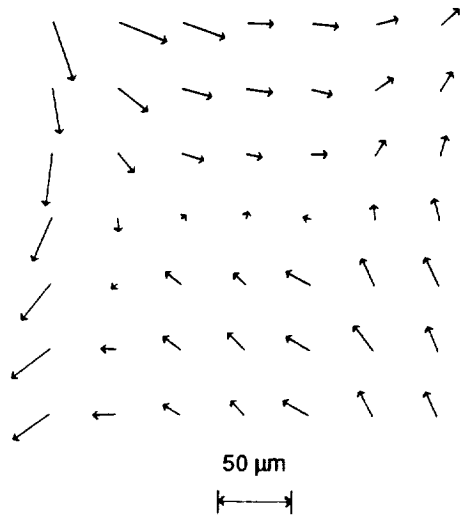

Figure 7. Residuals of CCD camera system from translation stage.

A source of error that is difficult to estimate and that is not considered here is due to the jagged edges of the bullet hole in which case the computed centroid may not indicate the true center. Note that for the laboratory tests with the 2-D translation stage, a single bullet hole was used so that this potential

source of error (jagged holes that vary from shot to shot) was not present.

In addition to the above repeatability and bias error tests, simple lighting tests were also conducted in which the overhead fluorescent lights were turned on for some data acquisition and turned off for others. The bullet hole was not moved during these tests. The illumination then consisted of either the direct lighting only or the direct lighting plus the overhead fluorescent lights. An approximate 50-μm variation was found as a result of this lighting difference (which is a much greater lighting difference than expected at the ballistics range). These tests point out the need for relatively constant and uniform illumination during a shooting session. Note that it may be possible to implement other location algorithms (such as the best fit to a circle) that may be less susceptible to target jaggedness or gross lighting variations (such as might occur at an outdoor range).

Concluding Remarks

A system consisting of a charge-coupled-device (CCD) camera, computer-controlled video digitizer, and software to automate the measurement has been developed for locating bullet holes in targets at the ballistics range at the Langley Research Center. An analysis of the potential errors and a technique for calibration of the system have been presented. Laboratory tests have shown that the long-term (1-hr) repeatability of the system is 4 μm (one standard deviation), and the maximum expected bias error, verified by comparisons with a two-dimensional translation stage, is less than 50 μm.

NASA Langley Research Center
Hampton, VA 23665-5225
June 29, 1990

Appendix

Error Considerations

The basic measurement concept is to replace the true scales (eqs. (4)), that vary with X with two fixed scales (eqs. (5)) found by calibration. The theoretically estimated error in the basic measurement concept is presented in the appendix for the expected geometry at the ballistics facility. Also presented are error estimates due to camera placement, misalignment of the paper target to the plane used for calibration, spacing of the calibration targets, measurement errors of the image and object planes, and optical lens distortion.

Error in Using Two Fixed Scales

The basic measurement concept of replacing the true scale that varies with X with two fixed scales can be tested by computing the errors in using equations (5) instead of equations (4). These errors are depicted in figure 8 for the following expected conditions at the ballistics facility: $X_c = 0.3$ m, $Z_c = 2.5$ m, $f = 150$ mm, $\Delta X = \Delta Y = 25$ mm. From the values of X_c and Z_c, ϕ is computed to be 6.84°. The computed values for the image distance c and the on-axis scale are 159.5 mm and 15.8, respectively, assuming that the camera is focused on the origin.

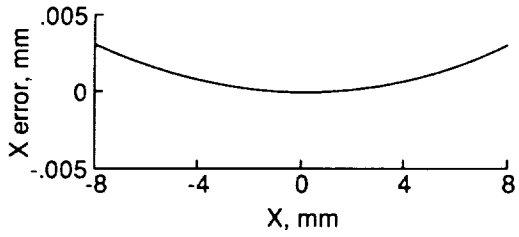

(a) X error versus true X.

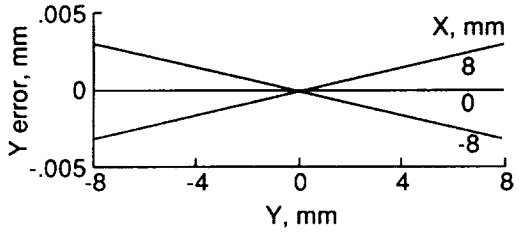

(b) Y error versus true Y.

Figure 8. X- and Y-coordinate errors in object plane versus true X and Y, respectively.

The true scales, S_Y and S_X computed from equations (2) and (3), respectively, were used to determine the image coordinates from equations (4) for the simulated calibration to determine S_{Xc} and S_{Yc}. The true image coordinates from equations (4) were then used in equations (5) to determine the measured object plane coordinates X' and Y' and the errors computed as $X' - X$ and $Y' - Y$ over the object field. The error in figure 8 is plotted over ±8 mm, the expected extent of shot dispersion in a shooting session. In figure 8(a) the X error (given in millimeters) that is independent of Y is plotted against the true X value. In figure 8(b) the Y error (given in millimeters) is plotted against the true Y value for $X = -8, 0$, and 8 mm. The largest error occurs at the edge of field, and for X or Y it is only 3.0 μm. It thus appears adequate, at least for this example, to replace the true scales that vary with X with the two fixed scales found by calibration.

Error Dependence on Offset Angle

It is next determined how small the camera angle to the XY-plane (ϕ) must be kept to avoid excessive error and how the error varies with ϕ. The X and Y errors versus ϕ are plotted in figure 9 for a point located at $X = Y = 8$ mm on the object plane. For this plot, the distance from the camera perspective center to the origin (D_o) was kept at 2.5 m to maintain a constant scale on axis, and the calibration scales were recomputed at each angle before computing the error. The X and Y errors for this plot were equal to within 0.023 μm and are plotted as one line. Over this range of ϕ the error is approximately linear with a slope equal to 0.44 μm/deg. Thus, for ϕ less than 10°, the error at the edge of field would be less than 4.4 μm.

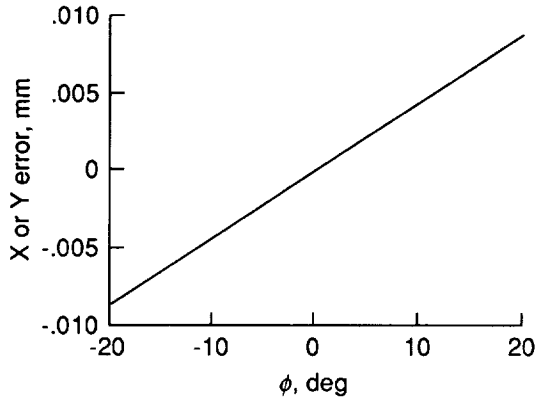

Figure 9. X or Y error in object plane versus ϕ (angle between camera optical axis and normal to object plane).

Error Dependence on Alignment of Paper Target

Another concern for the measurement process was that the paper target might not be positioned exactly in the same plane as that used for calibration. This could be due to a translation or rotation of the paper target with respect to the calibration plane. First consider that the paper target and calibration planes are separated by ΔZ (the Z difference between the calibration and object planes), but they are still parallel. The error due to this difference ΔZ is plotted in figure 10 for the same conditions as those in figure 8. The X and Y errors are equal to within 0.01 μm and are plotted as one line. For figure 10 S_{Xc} and S_{Yc} were computed with $Z_c = 2.5$ m; the object plane was then translated to $Z_c + \Delta Z$ and the image coordinates x, y were computed for an object at $X = Y = 8$ mm. Equations (5) were then used to compute the expected object plane coordinates from which 8 mm was subtracted to yield the error as a function of ΔZ. This error is approximately linear with a slope of 3.2 μm/mm. The alignment error ΔZ can be made less than 0.1 mm by using a feeler gauge (such as a piece of paper) to locate the paper target and calibration planes to the same reference surface, thus resulting in an expected error of less than 0.32 μm at the edge of field.

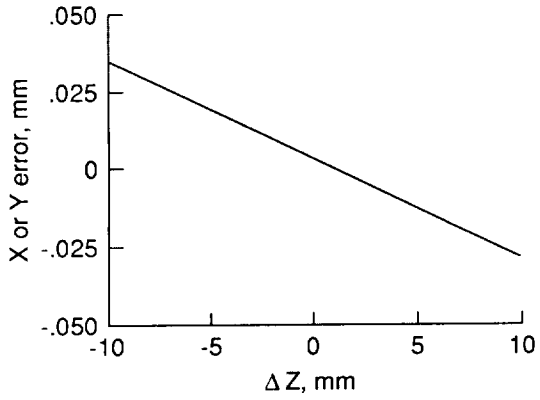

Figure 10. X or Y error versus ΔZ (the Z difference between the calibration and object planes).

The error introduced by rotation about the Y-axis of the paper-target object plane with respect to the calibration plane is presented in figure 11 for the conditions of figure 8. The calibrated scales S_{Xc} and S_{Yc} were computed for $\phi = 6.84°$. The camera angle ϕ was then incremented by $\Delta\phi$ before computing the image plane coordinates for use with equations (5) and the true X,Y values to compute the error. The X error $(X' - X)$ is approximately 16 μm/deg and the Y error $(Y' - Y)$ is approximately 0.45 μm/deg for small changes about $\phi = 6.84°$. Again, the difference in tilt angle can be held to 0.1° by using a feeler gauge to align the paper target and calibration planes and assuming that a height difference of 0.1 mm over 50 mm can be detected. This misalignment results in an expected error of 1.6 μm.

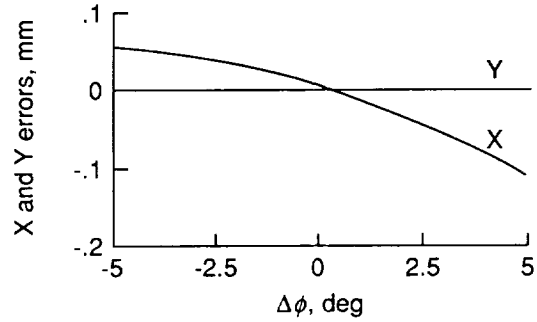

Figure 11. X and Y errors versus $\Delta\phi$ with calibration plane rotation angle fixed.

Error Dependence on Calibration Targets

It is also desirable to know the error dependence on the spacing of the calibration targets along the X- and Y-axes used to determine S_{Xc} and S_{Yc}. The effect of the spacing of the calibration targets is presented in figure 12 where the X error at the edge of a 16- by 16-mm object field ($X = Y = 8$ mm) is plotted against the spacing of the calibration targets for the same conditions as those for figure 8. The Y error is independent of the spacing of the calibration targets in the Y-direction since S_Y is independent of Y. The X error changes slightly (approximately 0.1 μm) as the calibration target spacing is increased to span the field of view.

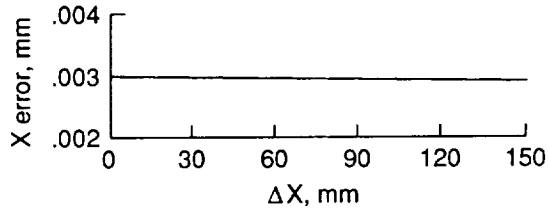

Figure 12. X error versus ΔX (spacing of calibration targets). Error in Y-coordinate is independent of ΔY.

Up to this point the errors associated with experimental measurements of length in the object or image plane have been ignored. Errors in experimentally determining the object and image plane separations of the calibration targets lead to bias errors in S_{Xc} and S_{Yc}. (See eqs. (6).) The separations of the calibration targets for this study were measured with an optical monocomparator that has a resolution of

1 μm and an uncertainty of less than 5 μm, thus resulting in an estimated error of 7 μm for the object plane separation. Using the above conditions where the object plane separation of the calibration target is 25 mm and the nominal scale is 15.8, the resulting error at the edge of a 16- by 16-mm object field is 2.2 μm because of object plane error in the spacing of the calibration targets. Even after distortion corrections are made, additional image plane distortions on the order of 1 μm result for CCD cameras (ref. 1) that can lead to an error in image plane separation of 1.4 μm during calibration. This image plane error during calibration can cause an object plane error of 7.0 μm at the edge of field.

Error Dependence on Residual Image Plane Distortion

Even with no other sources of error and a perfect calibration, the bullet hole location would still be in error because of the uncorrectable image plane distortion of 1 μm noted above for CCD cameras. The object plane error is related to the image plane error by the scale which (for the example used here) is approximately 15.8. Thus, the object plane error due to this 1-μm image plane error is approximately 16 μm and is the largest single source of error identified. This error is independent of the location of the bullet hole in the object plane.

Error Dependence on Optical Lens Distortion

Lens distortion is usually described by radial and decentering distortion terms. Radial distortion can exist even for a perfectly constructed lens; however, decentering distortion, which will be ignored in this analysis, arises from errors in construction and is generally much smaller than radial distortion. Radial distortion (δr), can be resolved into an odd-power series in r (the first-order radial distance on the image plane given by $(x^2 + y^2)^{1/2}$, where x and y are the first-order image coordinates). For many lenses the cubic term is a good approximation (ref. 2) to the distortion

$$\delta r = \sigma r^3 \tag{A1}$$

The third-order radial distortion coefficient (σ) has units of mm^{-2}. A tolerance of 1 percent is usually desired for δr when it is expressed as a percentage of the image height at the edge of field (ref. 2). For typical 2/3-in-format CCD sensors, such as those used in this report, the image plane is 8.6 (h) mm by 6.5 (v) mm so that the image height at the edge of field is 5.4 mm and a 1-percent tolerance for δr yields $\sigma = 3.4 \times 10^{-4}$ mm^{-2}. Measurements of σ (refs. 1 and 3) for several 25- and 50-mm focal-length video camera lenses have produced values of σ in the range of -1×10^{-4} mm^{-2} to -2×10^{-4} mm^{-2}, and more recent, unreported measurements at Langley have produced values of σ for 13-mm focal-length video camera lenses of -1×10^{-3} mm^{-2}.

Although there are several methods to determine the optical distortion including plumb line, test field, and analytic self-calibration (ref. 4), a simplification (based on the plumb line method) can be used to estimate the radial distortion without resorting to the more involved techniques. This simplified technique requires that only a single straight line or edge be located near the edge of field, and thus a quick estimation of σ can easily be made.

The radial distortion δr from equation (A1) can be resolved into components in x and y on the image plane as

$$\left.\begin{aligned} \delta x &= \sigma r^2 x = \sigma x^3 + \sigma y^2 x \\ \delta y &= \sigma r^2 y = \sigma y^3 + \sigma x^2 y \end{aligned}\right\} \tag{A2}$$

The image of a straight line that is parallel to the y-axis of the image plane (for example) and located near the edge of field will be curved (fig. 13) and have an x-coordinate (x'), equal to $x + \delta x$, which varies quadratically with y as

$$x' = x + \sigma x^3 + \sigma y^2 x \tag{A3}$$

The sagitta (sag) of the image of the straight line at y is given simply by

$$\text{sag} = \sigma y^2 x \tag{A4}$$

Now, x and y in equation (A4) are the undistorted first-order image coordinates that are unknown, but which can be approximated with the actual (distorted) image coordinates x' and y' to yield the following expression for the third-order radial distortion coefficient σ:

$$\sigma \approx \text{sag}/y'^2 x' \tag{A5}$$

Thus, it is relatively simple to obtain an estimate of σ by measuring the sagitta of the image of a straight line or edge at a particular x', y' at the edge of field. A negative value of σ indicates an inward distorting or barrel distortion, whereas a positive value indicates an outward distorting or pincushion distortion.

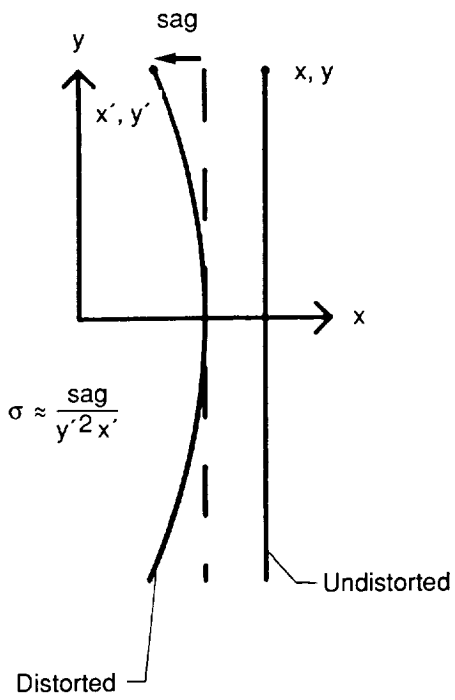

Figure 13. Estimation of third-order radial distortion σ by measuring sagitta (sag) of image of straight line.

Based on the above simplified technique, σ was found to be approximately 1.5×10^{-3} mm^{-2} for the lens used for this report. The scale found by calibration using equations (6) is in error because of this distortion. However, this error is partially compensated since for a positive σ, the calibrated scale will be smaller whereas the distorted-image data used in equations (5) to determine X' and Y' will be larger. In effect, the calibrated scale causes a linear term to be subtracted from the third-order distortion, thus reducing the effective distortion over the range of interest. At the edge of a 16- by 16-mm object field with a scale of 15.8, a calibration target spacing of 25 mm, and $\sigma = 1.5 \times 10^{-3}$ mm^{-2}, the combined error (calibration plus image plane) due to distortion is 4.4 μm at the object. This error can be reduced to 0.44 μm if σ can be determined to within ± 10 percent and be used to correct the image plane data.

Combining Elemental Error Sources

The elemental errors previously noted combine to produce bias (or systematic) error for a given setup. If the elemental errors are independent, then an estimate of the bias error can be made by taking the root sum square (rss) of the elemental error estimates. For a point at the edge of a 16- by 16-mm object field, the estimate of the bias error based on the rss of the various elemental errors identified above is 18.5 μm without correction for radial lens distortion and 17.9 μm with correction. It is thus apparent that correction for radial lens distortion causes little improvement because of the use of only the central portion of the image area and the partial compensation of the calibration. Distortion correction becomes more critical in situations where the majority of the image area is used (ref. 1). If the above calculations are repeated for an object field twice as large (32 mm by 32 mm), the estimated bias error becomes 26.9 μm without distortion correction and 25.1 μm with distortion correction.

References

1. Burner, A. W.; Snow, W. L.; Goad, W. K.; and Childers, B. A.: A Digital Video Model Deformation System. *ICIASF '87, IEEE Catalog No. 87CH2449-7*, Inst. of Electrical and Electronics Engineers, Inc., c.1987, pp. 210–220.
2. Kingslake, Rudolf: *Lens Design Fundamentals*. Academic Press, 1978.
3. Burner, A. W.; Snow, W. L.; and Goad, W. K.: Close-Range Photogrammetry With Video Cameras. *Technical Papers—51st Annual Meeting ASP, Vol. 1*, American Soc. of Photogrammetry, c.1985, pp. 62–77.
4. Slama, Chester C., ed.: *Manual of Photogrammetry, Fourth ed.* American Soc. of Photogrammetry, c.1980.

NASA
National Aeronautics and Space Administration

Report Documentation Page

1. Report No.	2. Government Accession No.	3. Recipient's Catalog No.
NASA TM-4197		

4. Title and Subtitle	5. Report Date
Video Camera System for Locating Bullet Holes in Targets at a Ballistics Range	August 1990
	6. Performing Organization Code
7. Author(s)	8. Performing Organization Report No.
A. W. Burner, D. R. Rummler, and W. K. Goad	L-16772
	10. Work Unit No.
9. Performing Organization Name and Address	505-61-01-05
NASA Langley Research Center Hampton, VA 23665-5225	11. Contract or Grant No.
12. Sponsoring Agency Name and Address	13. Type of Report and Period Covered
National Aeronautics and Space Administration Washington, DC 20546-0001	Technical Memorandum
	14. Sponsoring Agency Code

15. Supplementary Notes

16. Abstract

A system consisting of a single charge-coupled-device (CCD) video camera, computer-controlled video digitizer, and software to automate the measurement has been developed for locating bullet holes in targets at a ballistics range at the Langley Research Center. The camera/digitizer system is a crucial component of a highly instrumented, indoor 50-m rifle range that supports the development of wind-resistant ultramatch ammunition. The system was designed to take data rapidly (10 sec between shots) and automatically with little operator intervention. The system description, measurement concept, and procedure are presented along with laboratory tests of repeatability and bias error. The long-term (1-hr) repeatability of the system was found to be 4 μm (one standard deviation) at the target, and the bias error was found to be less than 50 μm. An analysis of the potential errors and a technique for the calibration of the system are presented.

17. Key Words (Suggested by Authors(s))
Ballistics
Charge-coupled-device (CCD) camera
Video

18. Distribution Statement
Unclassified Unlimited

Subject Category 35

19. Security Classif. (of this report)	20. Security Classif. (of this page)	21. No. of Pages	22. Price
Unclassified	Unclassified	15	A03